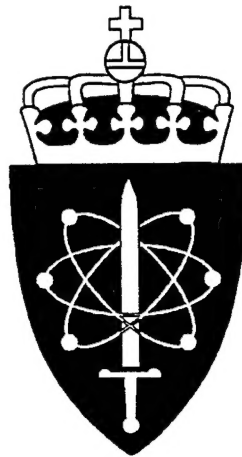


REPORT DOCUMENTATION PAGE			Form Approved OBM No. 0704-0188	
Public reporting burden for this collection of information is estimated to average 1 hour per response, including the time for reviewing instructions, searching existing data sources, gathering and maintaining the data needed, and completing and reviewing the collection of information. Send comments regarding this burden or any other aspect of this collection of information, including suggestions for reducing this burden, to Washington Headquarters Services, Directorate for Information Operations and Reports, 1215 Jefferson Davis Highway, Suite 1204, Arlington, VA 22202-4302, and to the Office of Management and Budget, Paperwork Reduction Project (0704-0188), Washington, DC 20503.				
1. AGENCY USE ONLY (Leave blank)		2. REPORT DATE June 1995		3. REPORT TYPE AND DATES COVERED Proceedings
4. TITLE AND SUBTITLE Discussions accompanying presentation of transparencies			5. FUNDING NUMBERS Job Order No. 735906A5 Program Element No. Project No. Task No. Accession No.	
6. AUTHOR(S) Donald R. Johnson				
7. PERFORMING ORGANIZATION NAME(S) AND ADDRESS(ES) Naval Research Laboratory Oceanography Division Stennis Space Center, MS 39529-5004			8. PERFORMING ORGANIZATION REPORT NUMBER NRL/PP/7332--98-0031	
9. SPONSORING/MONITORING AGENCY NAME(S) AND ADDRESS(ES) Office of Naval Research 800 North Quincy Street Arlington, VA 22217-5000			10. SPONSORING/MONITORING AGENCY REPORT NUMBER	
11. SUPPLEMENTARY NOTES NDRE Workshop on Modeling Requirements for Water Mass Dynamics, Ice and River Transports in the Kara Sea, 26-30 June 1995, Tjome, Norway				
12a. DISTRIBUTION/AVAILABILITY STATEMENT Approved for public release; distribution is unlimited.			12b. DISTRIBUTION CODE	
13. ABSTRACT (Maximum 200 words) The Kara Sea contributes about 1/2 the fresh water inflow to the Arctic. This makes it extremely important from physical dynamics as well as from Arctic pollution concerns, especially since the drainage basins of the contributing rivers are industrialized. Vigorous mixing from tides inertial currents and winds spread the river outflow toward the west as well as toward the east as expected from fluid dynamics on a rotational earth. This westward spreading was confined in 1994 due to a relatively strong current along the slope of the Yamal Plateau. Flow along the eastern side of Novaya Zemlya was northward, instead of southward as expected. Flow around the northern tip of Novaya Zemlya appeared to be northwestward, instead of southeastward, into the Sea, as expected. However, without longer time series, this cannot be justified as characteristic, even over the short summer time. We need to better understand the pathways for spreading of Kara Sea fresh water into the rest of the Arctic.				
14. SUBJECT TERMS physical oceanography, Kara Sea, Arctic, inertial currents, Yamal Plateau, Novaya Zemlya, and pollution			15. NUMBER OF PAGES 30	
			16. PRICE CODE	
17. SECURITY CLASSIFICATION OF REPORT Unclassified		18. SECURITY CLASSIFICATION OF THIS PAGE Unclassified		19. SECURITY CLASSIFICATION OF ABSTRACT Unclassified
				20. LIMITATION OF ABSTRACT SAR



NDRE WORKSHOP

19980814 002

MODELING REQUIREMENTS

FOR WATER MASS DYNAMICS, ICE AND
RIVER TRANSPORTS IN THE KARA SEA

RICA HAVNA HOTEL, TJØME, NORWAY

26 – 30 JUNE 1995

DTIC QUALITY INSPECTED 1

NORWEGIAN DEFENCE RESEARCH ESTABLISHMENT

CONTENTS

List of participants

Group photo

K. Crane

Northern ocean inventories of radionuclide contamination: GIS efforts to determine the past and present state of the environment in and adjacent to the Arctic

1

T. A. Vinogradova and Y. B. Vinogradov

Mathematical modelling of the pollutant flow from the Arctic river watersheds

26

T. Paluszkievics, L. Hibler, M. Richmond, P. Farley,

D. Bradley and P. Becker

An assessment of the flux of radionuclide contamination through the Ob and Yenisei rivers and estuaries to the Kara Sea

49

V. V. Ivanov

The studies of the Kara mouth region, priorities of studies for the modeling of water mass dynamics, thermohaline and ice processes

70

D. R. Johnson

Discussions accompanying presentation of transparencies

85

Y. P. Doronin and V. V. Ivanov

Numerical modeling of water mass dynamics, thermohaline and ice processes in the Kara mouth region

112

Å. Skøelv and T. Wahl

NDRE satellite remote sensing activities in the Kara Sea in 1993 and 1994

124

Ye. O. Aksenov, Z. M. Gudkovich, S. P. Pozdnyshev and

D. A. Speransky

Numerical modelling of sea ice evolution with the purpose of ice forecasting from one to ten days in advance

136

R. H. Preller and A. Cheng

Modeling the dispersion of radioactive contaminants in the Arctic using coupled ice-ocean model

144

V. V. Ivanov

Inflow and spreading of river water in the Kara Sea, its multiyear and interannual variability

161

J. Carroll and I. H. Harms

The importance of sediment/water partition coefficients in modeling radionuclide dispersion in the Kara Sea

179

V. K. Pavlov

Modelling of the thermohaline water circulation of the Arctic Ocean

200

V. K. Pavlov, M. Yu. Kulakov, V. V. Stanovoy Modeling of the transport and transformation of pollutants in the Arctic Ocean	225
I. V. Polyakov A coupled sea ice-ocean model of the Arctic Ocean and the Kara Sea: Applications and perspectives	249
T. B. Løyning Convection processes at cold temperatures	263
Ye. O. Aksenov and K. A. Teitel'baum Analysis of interannual variability in anomalies of sea ice thickness in the Kara Sea in the observation data of polar stations	279
G. Evensen, W. P. Budgell, O. M. Johannessen and P. M. Haugan Numerical investigation of transport and dispersal of radioactive wastes in the Kara Sea	289
U. R. Aakenes RADAM-Aircraft launch self-mooring radioactivity sensors with duplex communication link	300
E. Nøst Current data from KAREX-94	310
C. Toro Nordic seas and the SEAWATCH system	326
H. Engedahl Hindcast simulations of ocean currents in the Norwegian coastal waters; Part 1: Model set up and sensitivity tests	335
E. A. Martinsen Hindcast of ocean currents. Summary report	368
B. Ådlandsvik Modelling examples of transport of water soluble radioactive waste	392
T. A. McClimans The use of laboratory models in the development, calibration and validation of numerical models	404

Donald R. Johnson

Discussions accompanying presentation of transparencies.

Figure 1: Bathymetry and postulated currents based upon the Northwind cruise of 1965. The Ob-Yenisey Delta (also called the Yamal Plateau) is a dominating feature of the bottom topography. It has a characteristic depth of less than 50 meters. The East Novaya Zemlya Trough reaches depths in excess of 300 m, but with a sill depth communicating to the Svyataya Anna Trough to the north of around 150 m. Postulated circulation (principally from water mass analysis) shows a flow from the rivers both toward the north and along the coast toward the east as expected. In the western side of the basin, there is a counterclockwise flow pattern, with northward flow along the edge of the delta and southward along Novaya Zemlya. Modified North Atlantic Water could be observed entering the Sea through the Kara Gate and around the northern tip of Novaya Zemlya. Flow was also seen entering the Sea from the Laptev Sea.

Figure 2: Salinity observed at the 10 meter level during the Northwind cruise in 1965. I have colored water with less than 30 parts per thousand of salt so that the 'fresher' water stream can be observed from the river entrances, across the delta toward the northeast and then northward out of the Kara Sea.

Figure 3: Ship track during the 1994 cruise. I have labeled the major rivers contributing to the Kara Sea, the Yenisey, Ob and Pechora. The Pechora contributes through the Kara Gate and, as of now, it is not clear how much it contributes and what factors influence this level of contribution. I have also labeled two sections that I will be discussing in my presentation (Novaya Zemlya (NZ) to Dickson and Dickson to 'West').

Figure 4: During the cruise in 1994, 9 current meter moorings were deployed. Eight were retrieved at the end of the cruise and one left to overwinter in the trough. The symbols colored red had both bottom and surface current meters on the moorings, and the green colored symbols had only bottom current meters.

Figure 5: This figure shows the location of hydrographic stations made with a CTD (conductivity, temperature, depth recorder). The CTD also had a fluorometer and a light transmission sensor on board. Since it will become important, I note that there is a lack of data in the middle of the 'V'.

Figure 6: Salinity at 5 meters depth measured at the hydrographic stations. You can see the station locations represented on this graph. In the upper right, there is a key for the color representation of salinity running from 10 to 32 parts per thousand. It is quite clear that the low salinity river water turns right and spreads both toward the north and toward the east, and flows on both sides of Sverdrup Island. The 'bending' toward the west may be partially attributed to the lack of data in the

central region and the tendency of the gridding program to fill-in the blank area.

Figure 7: Chlorophyll-a at 5 meters as determined by the fluorometer. note the heavy contribution from the Ob River, and again the indication of a northeastward flow but with spreading also into the interior.

Figure 8: Light transmission at 5 meters. In the key in the upper right hand corner of the transparency, it can be seen that the lowest light transmission at this shallow depth is around 40%, indicating strong sediment and biological loads of the rivers, especially the Ob.

Figure 9: Mean currents from the current meters, averaged over the period of deployment. The blue arrows indicate surface currents, and the red arrow indicate bottom currents. The largest current vector in the figure, on the upper slope of the delta, is 10 cm/s. Note the eastward flow along the coast, but the northwestward flow in the center/west of the river outflow. Also note the bottom return flow toward the rivers. But the bottom flow on the edge and outside of the delta, goes toward the north and east. These currents are very well aligned with topography.

Figure 10: Time series of near surface currents at the entrance to the Ob River estuary. The y-axis represents current speed in cm per second and the x-axis represents time in Julian days. The red line is the east component of current speed and the blue line is the north component. Note that the currents here are strongly dominated by the semi-diurnal tide with amplitudes exceeding 40 cm/s. The average current is only about 3 cm/s.

Figure 11: Time series of currents along the slope of the Yamal Plateau. The red line represents shallow components of the current and the blue line represents the deep components. The time series in the upper graph are the cross-topography components and the lower graph contains the along-topography components. Although tidal currents are well represented here also, especially in the surface currents (red lines), they are dominated by a sub-tidal component. Note also that at the end of the deployment, gale force winds began to blow. There is a strong amplification of currents both at the surface and at the bottom during this period showing barotropic behavior.

Figure 12: Since the semi-diurnal tide is 12.42 hours and the inertial period is 12.48 hours, we can expect a lot of energy in that particular period. For that reason, I have averaged the currents every 12.5 hours and displayed the individual vectors in this figure. This gives an indication of the suprisingly strong sub-tidal fluctuations in the surface currents. Note that the currents to the east of the rivers have mostly an eastward component, the central and westward currents are heavily scattered and more toward the northwest. This indicates that there should be strong horizontal mixing toward the west accompanying the advection

toward the east.

Figure 13: The strong variability can be demonstrated in this section of currents at 15 m, taken by the shipboard acoustic doppler current profiler (adcp). These are the 'raw' values taken during the ship transect from NZ to Dickson.

Figure 14: But if we take into account the 12.5 hour tides and inertial components, and average the adcp data over a 'running' 12.5 hours, the picture becomes much better. Of course, since the ship is moving during the averaging time, there is a space/time smear. Nevertheless, the picture is much improved of the near-surface circulation pattern and tends to confirm the general pattern from the moored current meters. There is an outflow along the coast and around the north side of Sverdrup Island. In the western side of the basin, there is a general northward drift. And around the northern tip of Novaya Zemlya, there is an outflow.

Figure 15: Short-term satellite tracked drifters were also released. The arrows alongside of the tracks show the drift directions. This also confirms the flow pattern as seen by the other systems, plus shows an inflow through the Kara Gate.

Figure 16: Sea surface temperature and salinity along the track from Dickson to 'West' across the river entrances into the trench area (section location shown on Fig. 3).

Figure 17: Bottom topography measured by the Precision Depth Recorder onboard. This figure, together with Fig. 16 shows the very strong salinity front that occurs to the west of the river entrances. The front appears to be situated over the edge of the delta.

Figure 18: Sea surface temperature and salinity along the track from NZ to Dickson (see fig. 3). Here front is more smeared out, and may actually be a double front.

Figure 19: Bottom topography to accompany fig. 18. Also shows alignment of salinity front with edge of delta.

Figure 20: Scales. In order to understand something of the placement of this salinity front, I resort to scaling. In this figure, I show scales for a water column in front of the rivers. With the Coriolis parameter, vertical density difference and depth as indicated, the internal radius of deformation can be calculated as about 37 km. This is much too short for these fronts, which appear at about 170 km from the rivers. But if we take a horizontal mixing coefficient which ranges from e^{+06} to e^{+08} , then the time scale for spreading that distance ranges from 300 to 30 days. With vigorous mixing, the 30 day time scale would be adequate. This would mean that the front may be the result of halting of spreading by the topographically trapped current that we have seen on the edge of the delta.

Figure 21: In order to investigate the winds as a force responsible for the spreading, I do a vector correlation between winds and sub-tidal currents at all of the near-surface moorings. From this figure, we can see a suprisingly high correlation (above .6) with a rotation of the currents to the right of the winds in all cases as expected from Coriolis. Although the number of points involved in the statistics is small, nevertheless, the pattern seems very clear.

Figure 22: In this figure, I show the location of the correlation values. Clearly the higher correlation is outside of the plume and in the region of the west and northwestward spreading. This gives us an indication that the winds are a major driving force in spreading and horizontally mixing the river plumes.

Figure 23: In this figure, I show a salinity and temperature profile (pressure/depth downward from 0 to 35 meters, and salinity running from 10 to 35 parts per thousand). From this picture is clear that there is a strong halocline of over 15 parts per thousand over less than 10 meters at a location 100 km north of the river. With this strong vertical inhibition to the downward flux of momentum, the horizontal mixing by winds can be very vigorous.

Figure 24: Conclusions.

continental shelf (Fig. 1). The islands of Franz Joseph Land and Novaya Zemlya and the imaginary line connecting them separate the Barents Sea from the Kara Sea. The southern limits are the West Siberian Lowlands and the Taymur (Taymyr) Peninsula. The eastern limits are the

islands of Severnaya Zemlya. The northern limits are defined by the imaginary line connecting the northernmost islands of Franz Joseph Land and Severnaya Zemlya, at approximately $81^{\circ}30'$ north latitude.

The area of the Kara Sea is 851,000 km² with

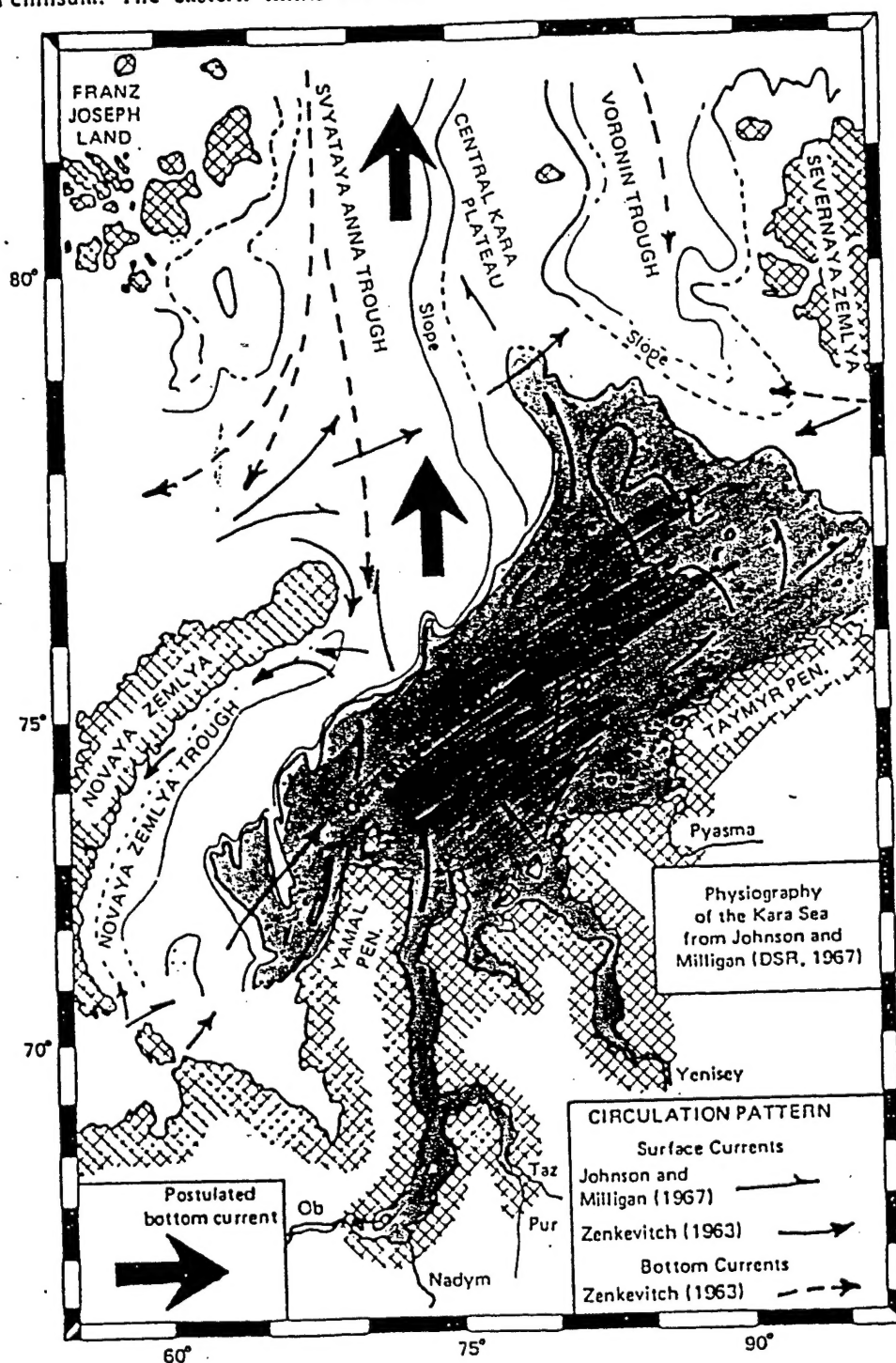
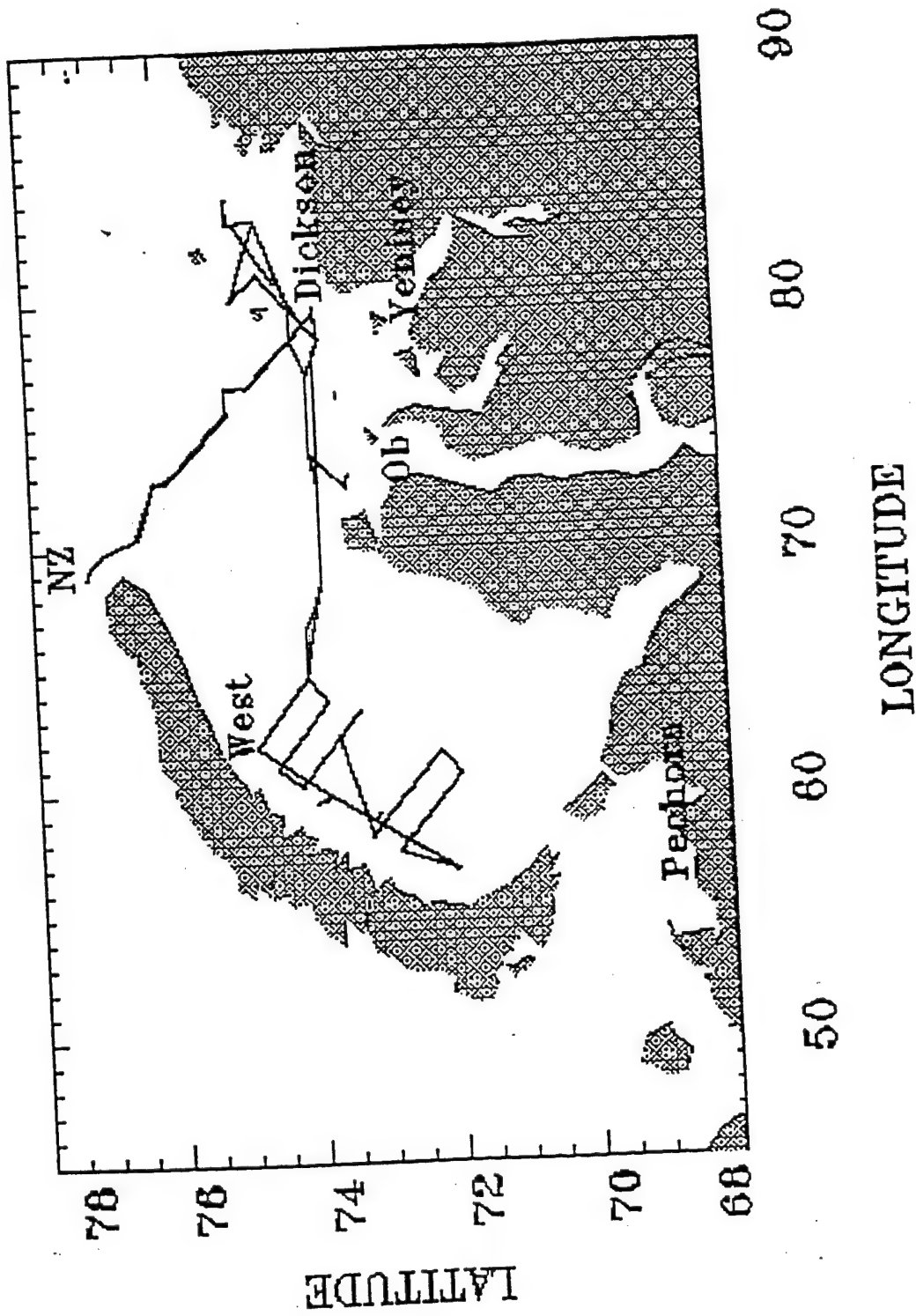


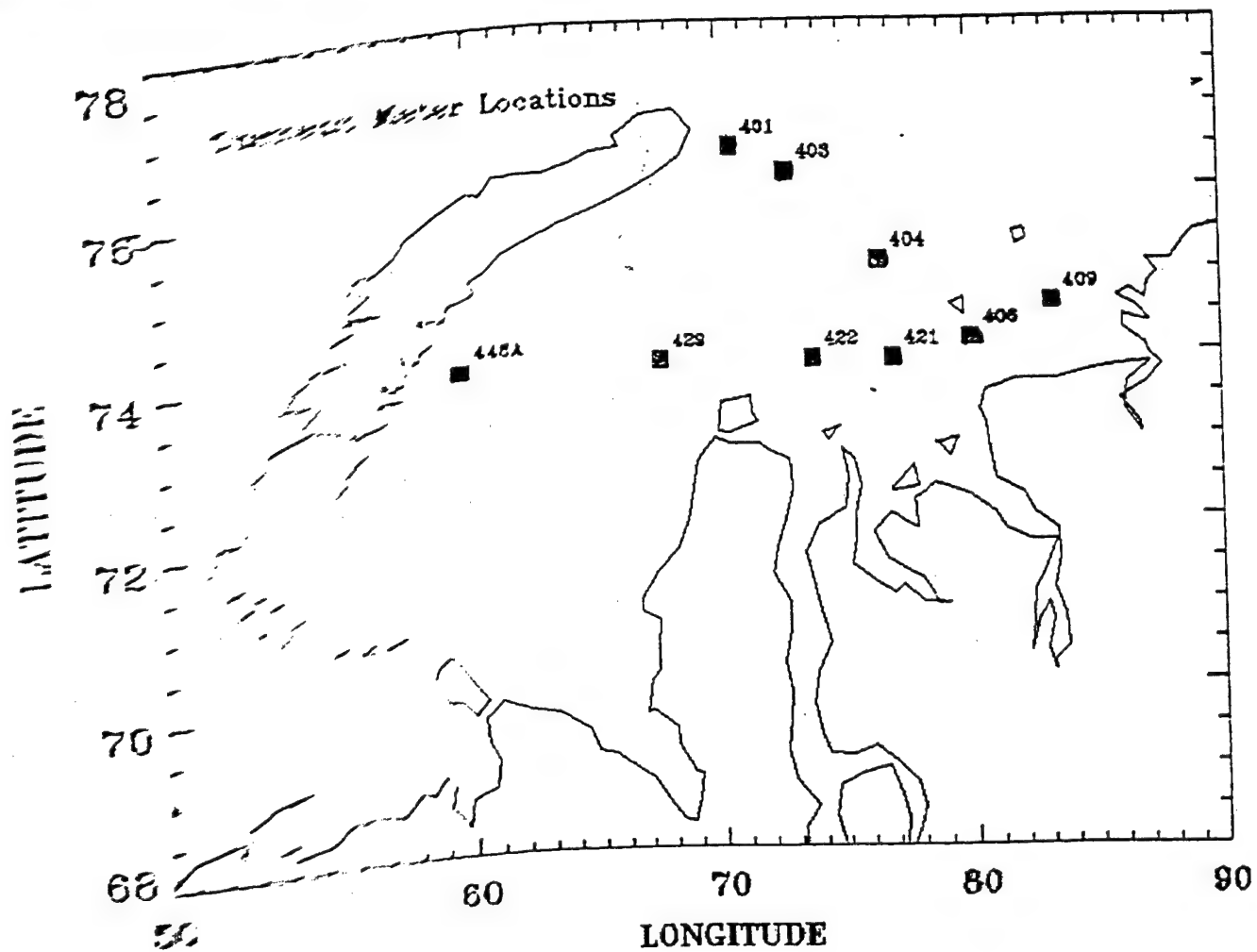
Fig. 2. Physiography and currents of the Kara Sea. Physiography from Johnson and Milligan (1967) based on data collected from the *Northwind*. The large arrow indicates the position of the north-flowing current postulated from data contained in this study.



Fig. 9. Isohaline contours at a depth of 10 m. Dots show location of *Northwind* Stas. The location of the profile in the lower right is shown by a heavy black line. Vertical exaggeration of the profile is 660:1. 34.5‰ salinity water is Atlantic water (COACHMAN and BARNES 1961). The circulation is shown by arrows on Fig. 1.

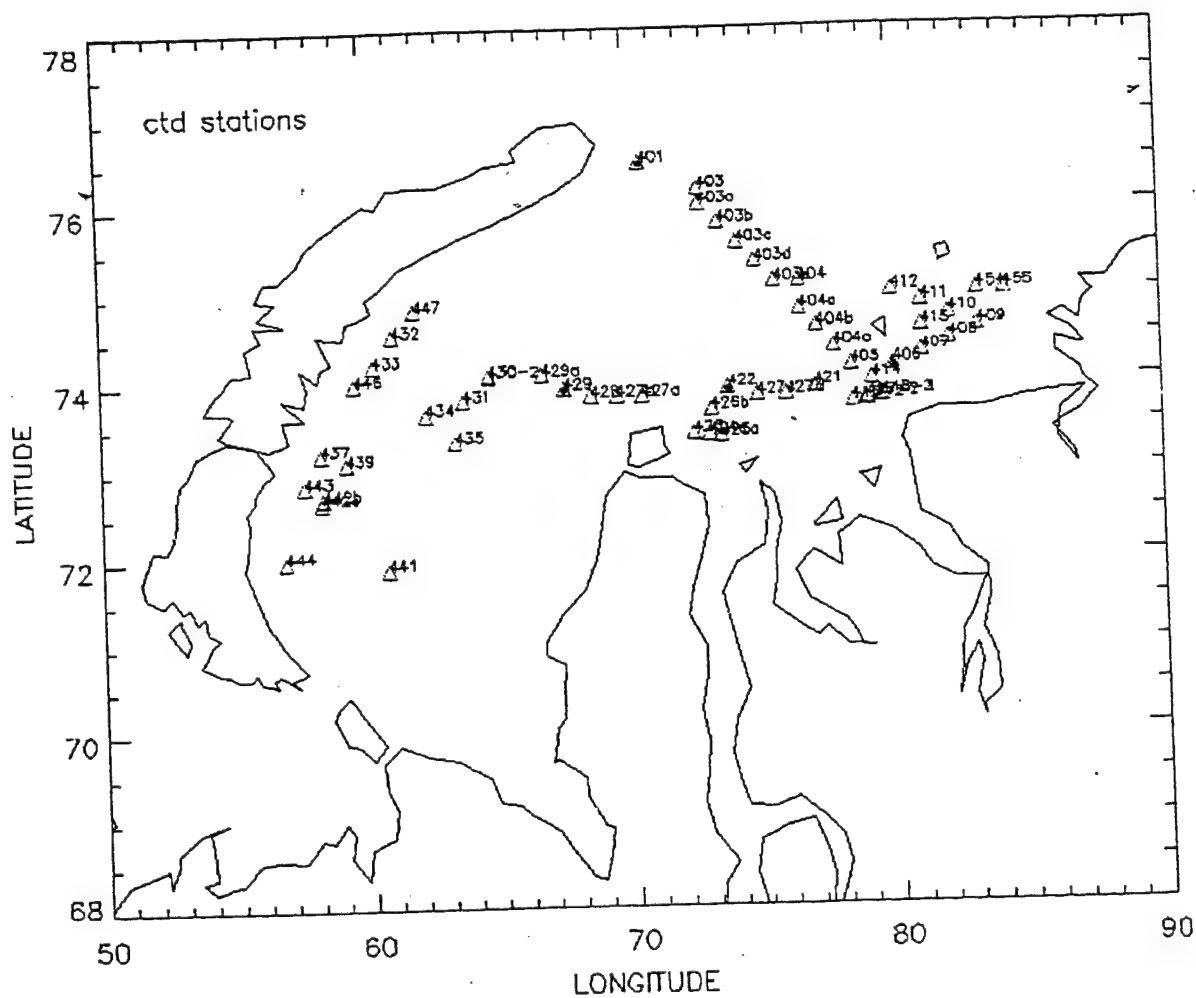


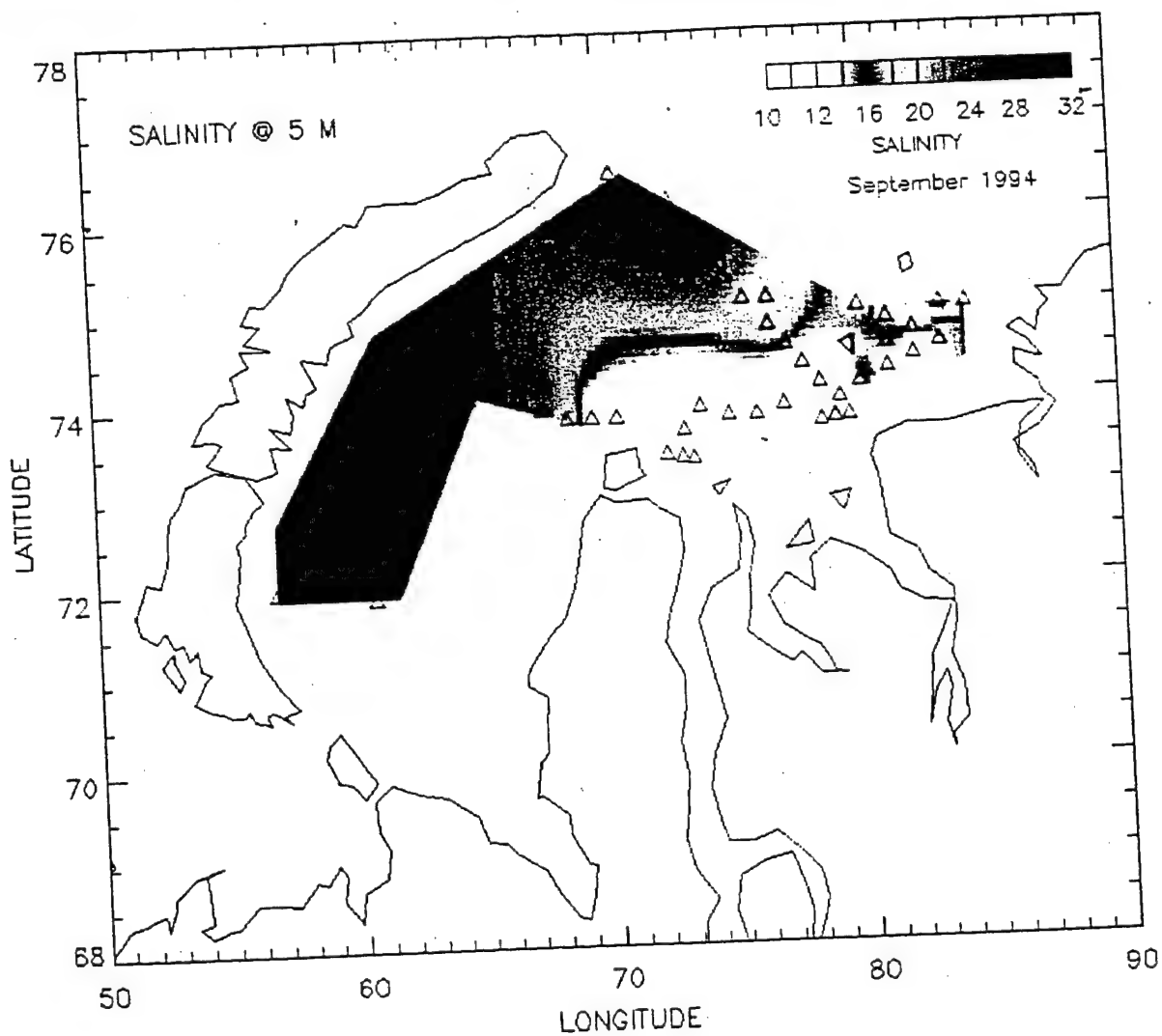
Ship Track 1994

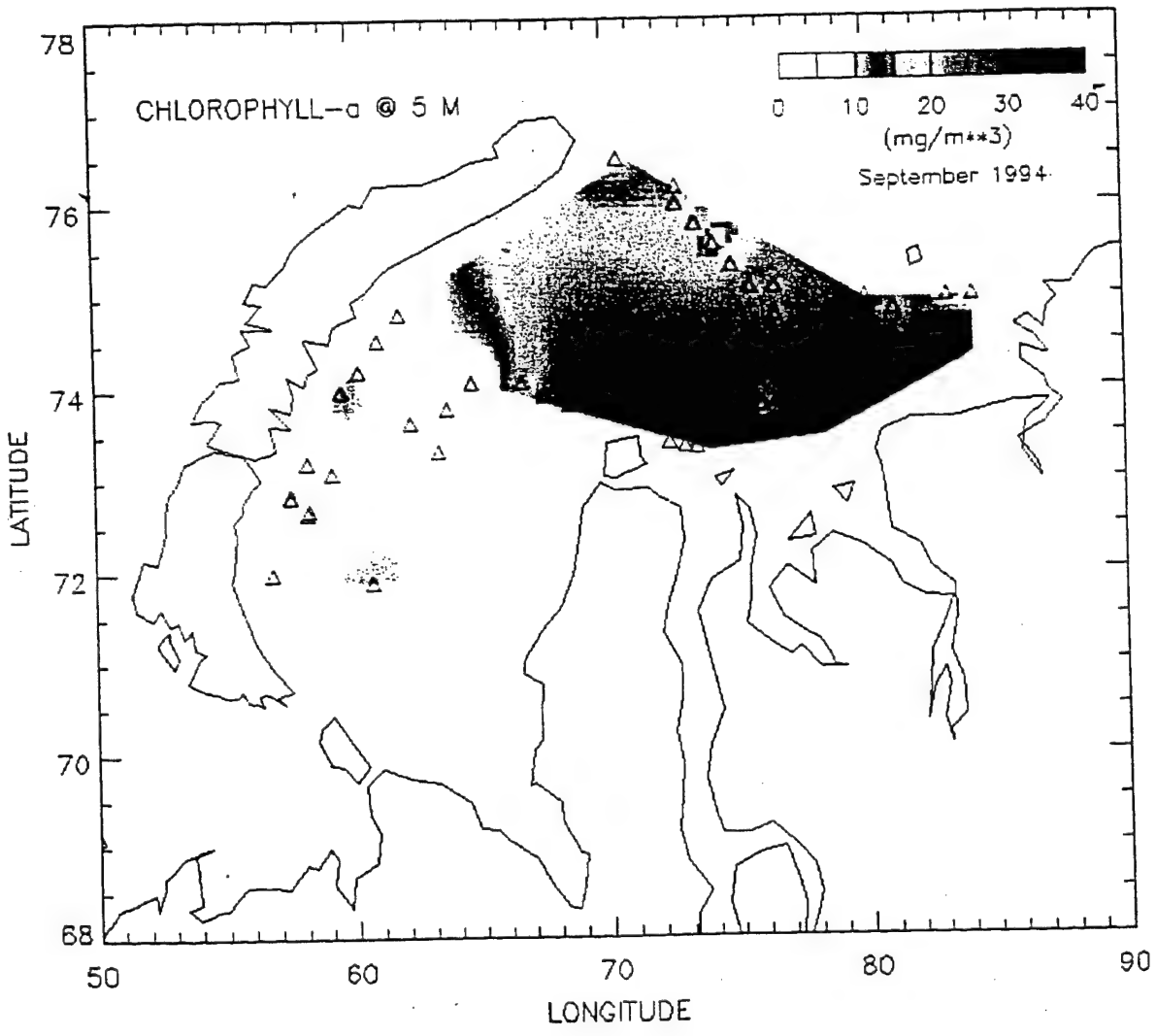


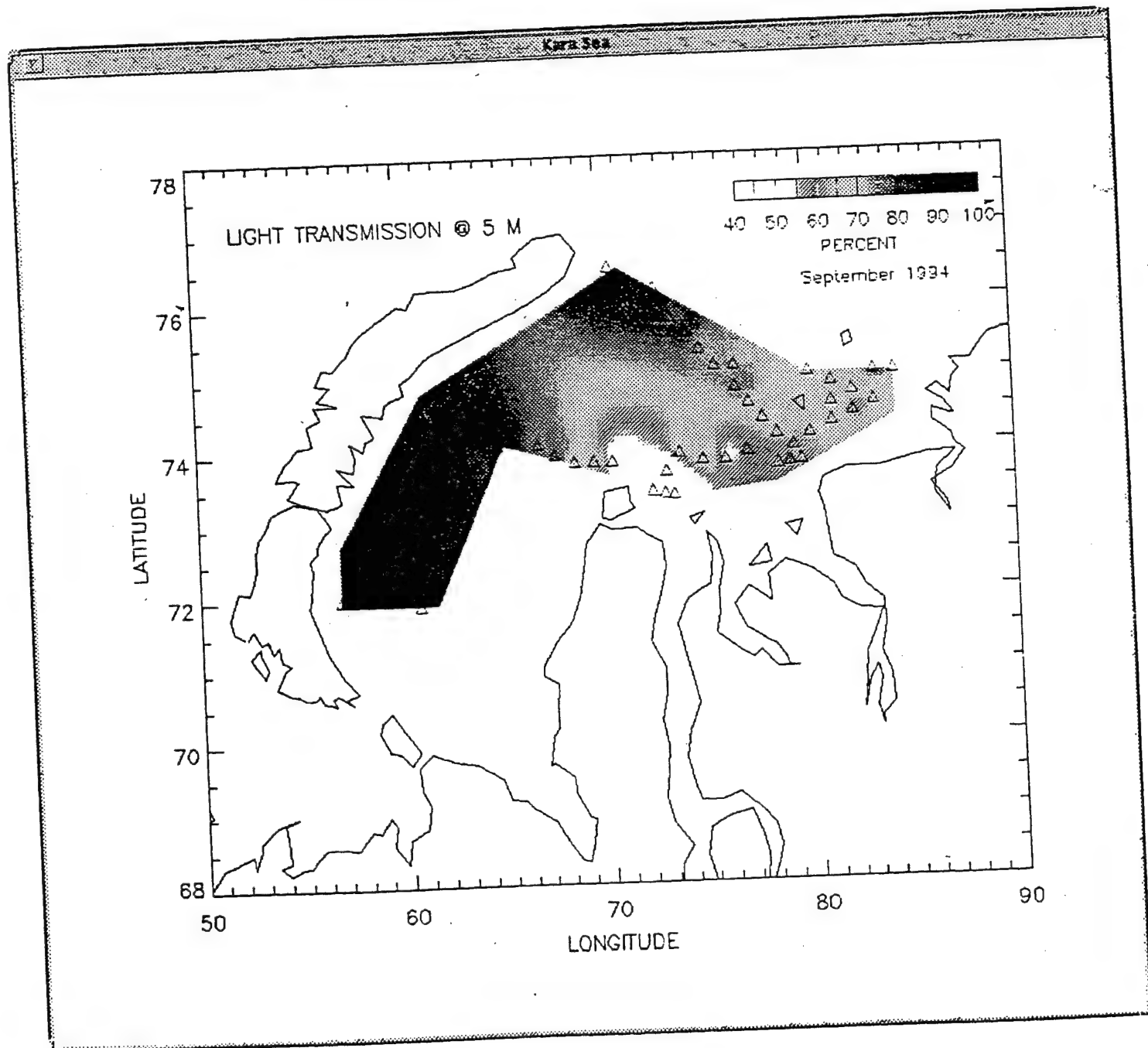
- - Surface & Bottom
- ▢ - Bottom only

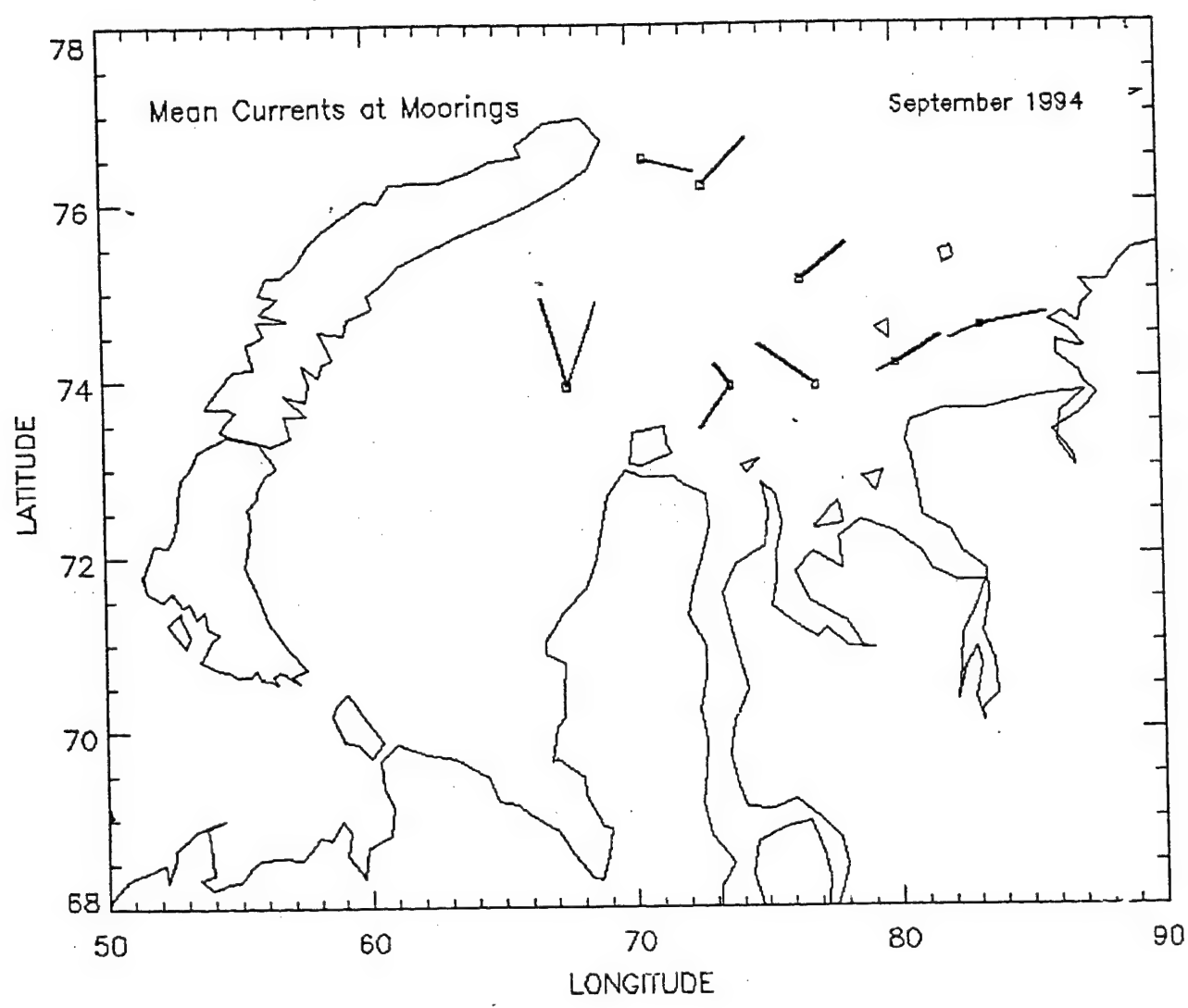
Kara Sea 54





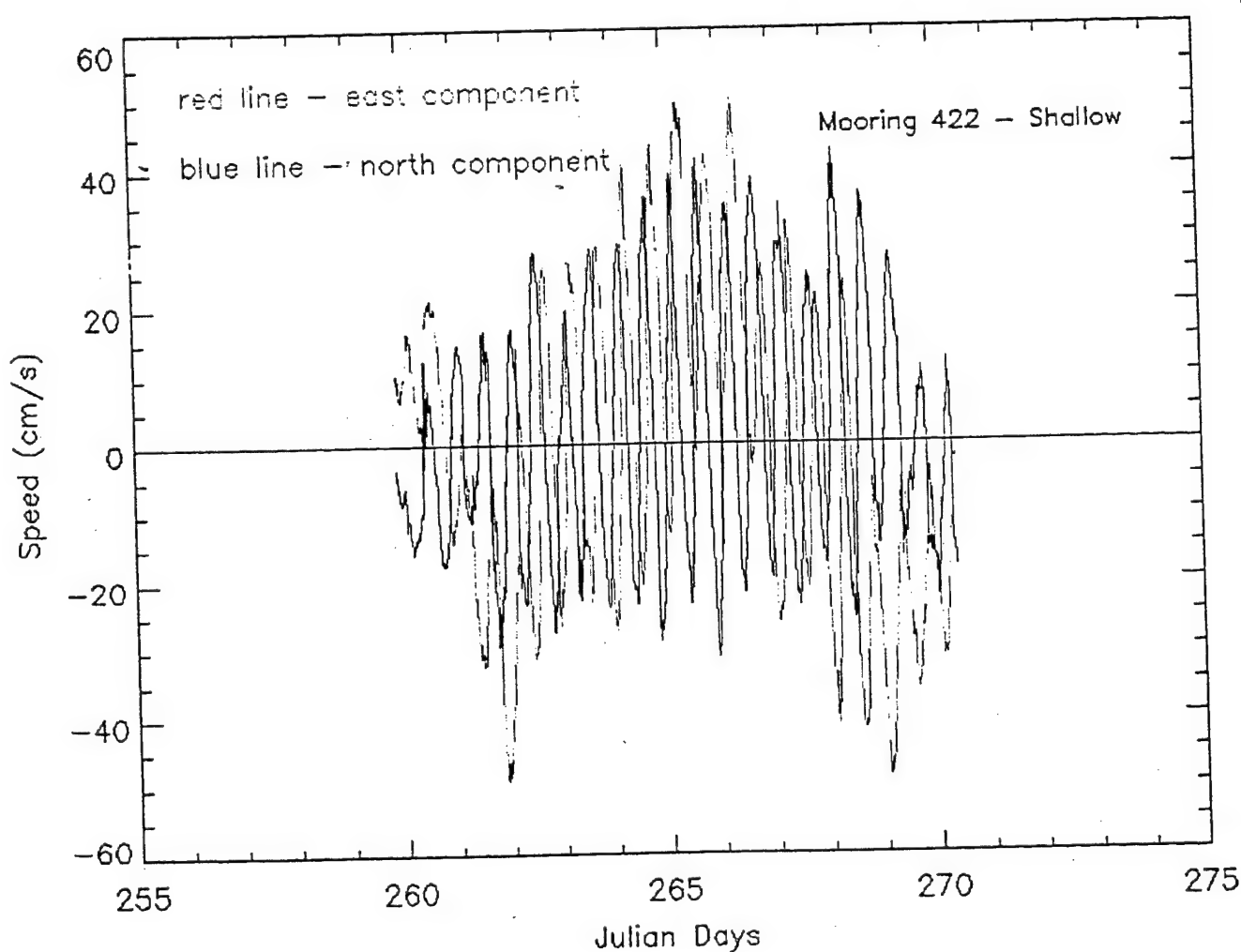


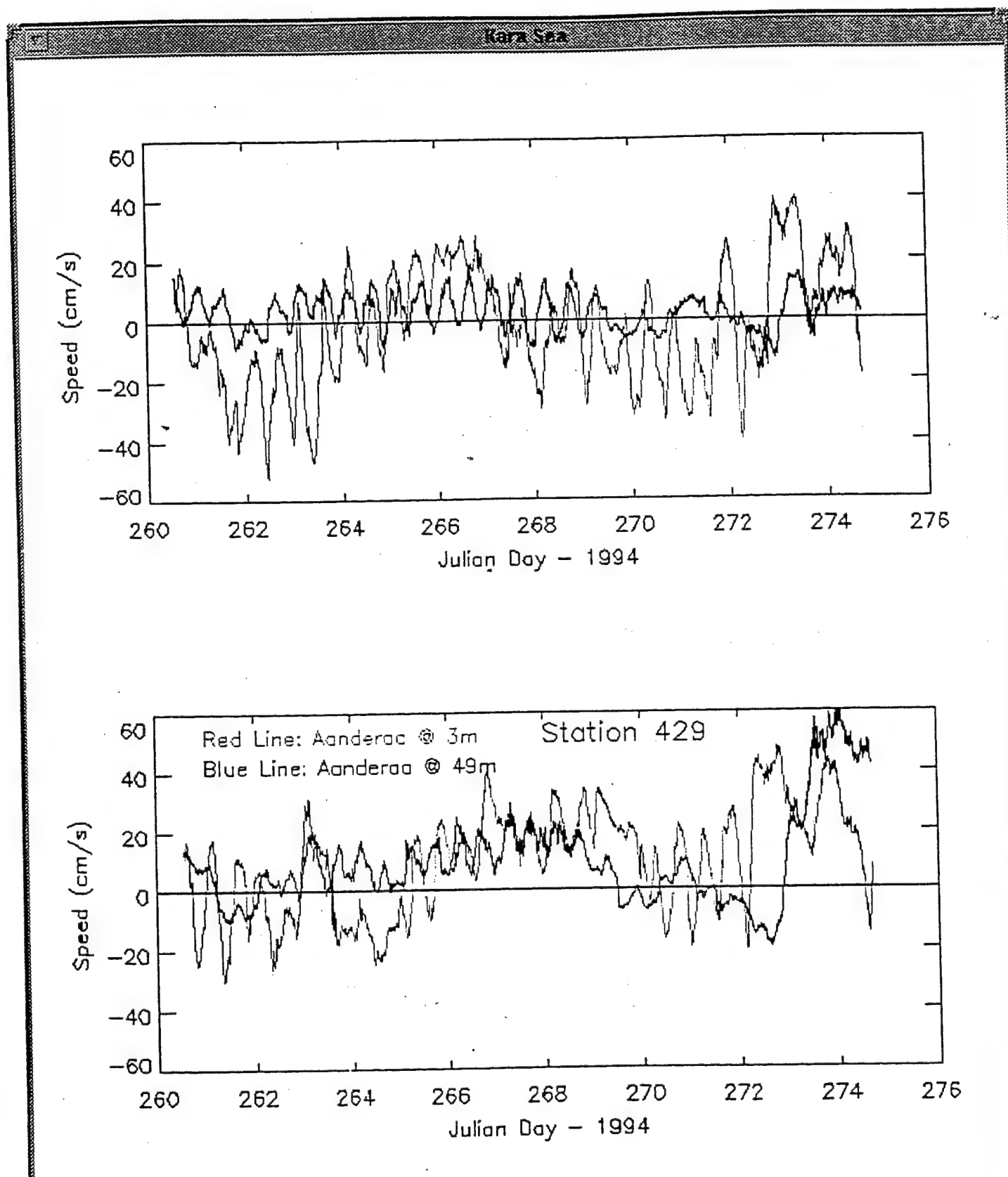


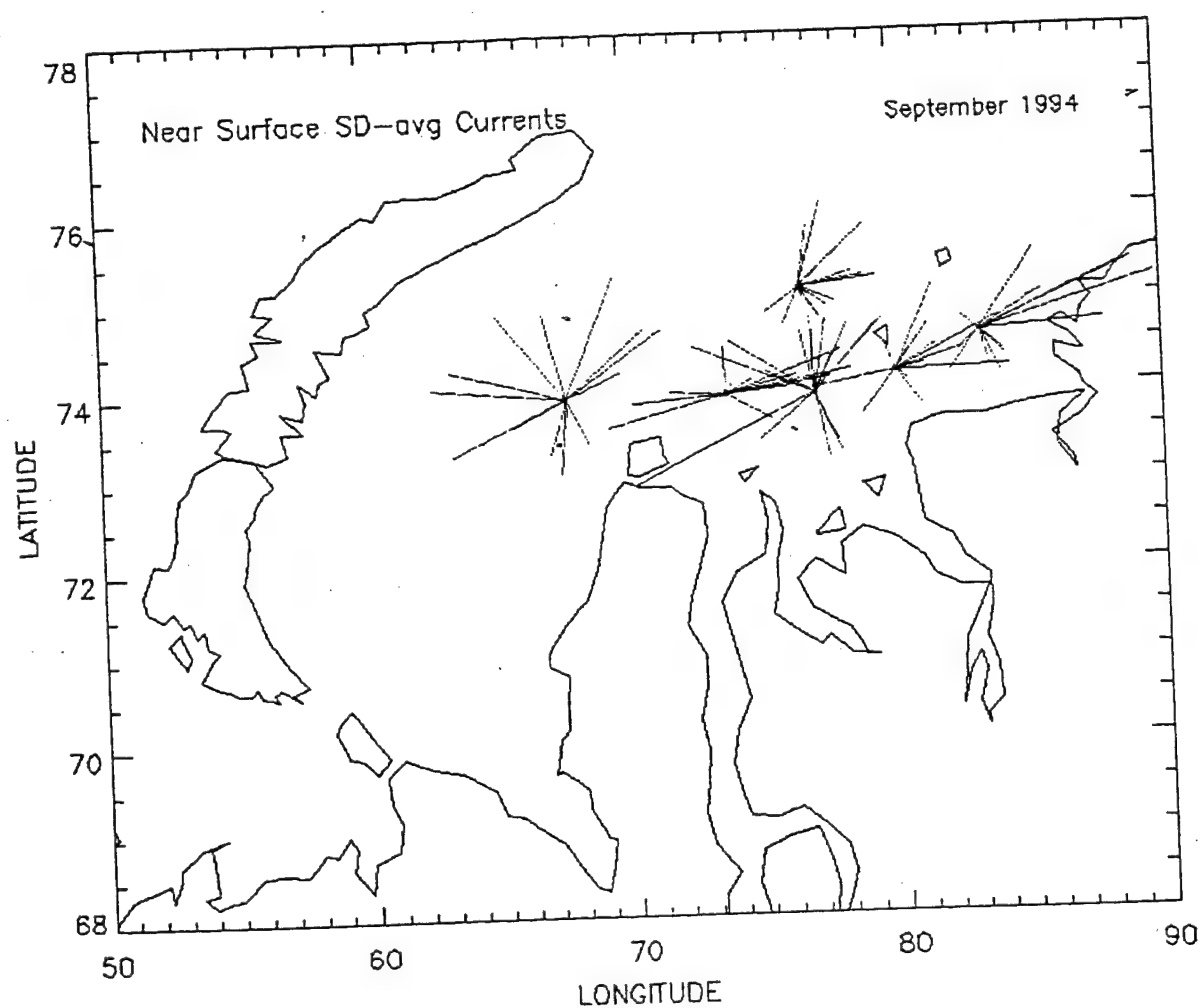


— Bottom
— Surface

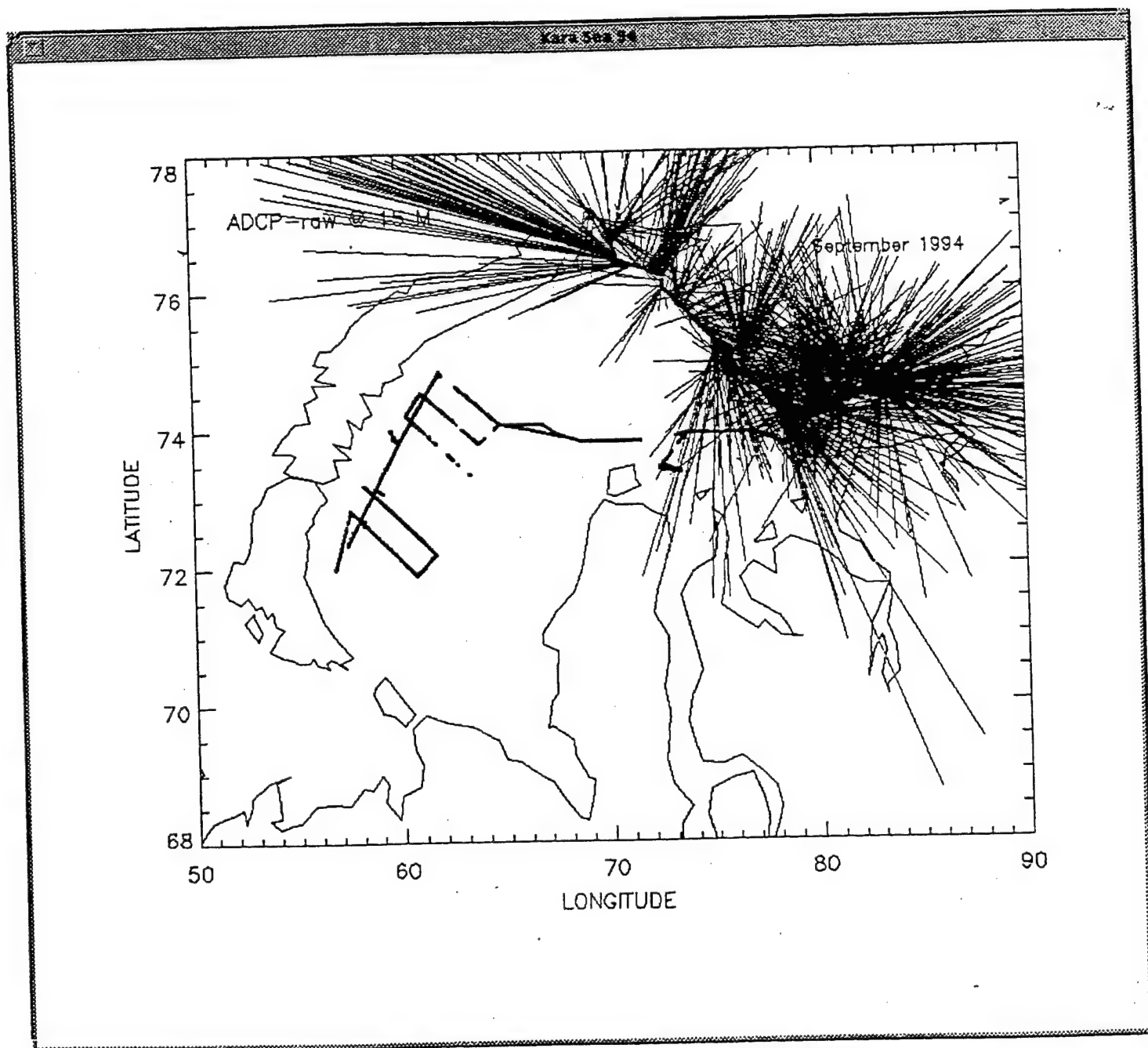
WAVE 2



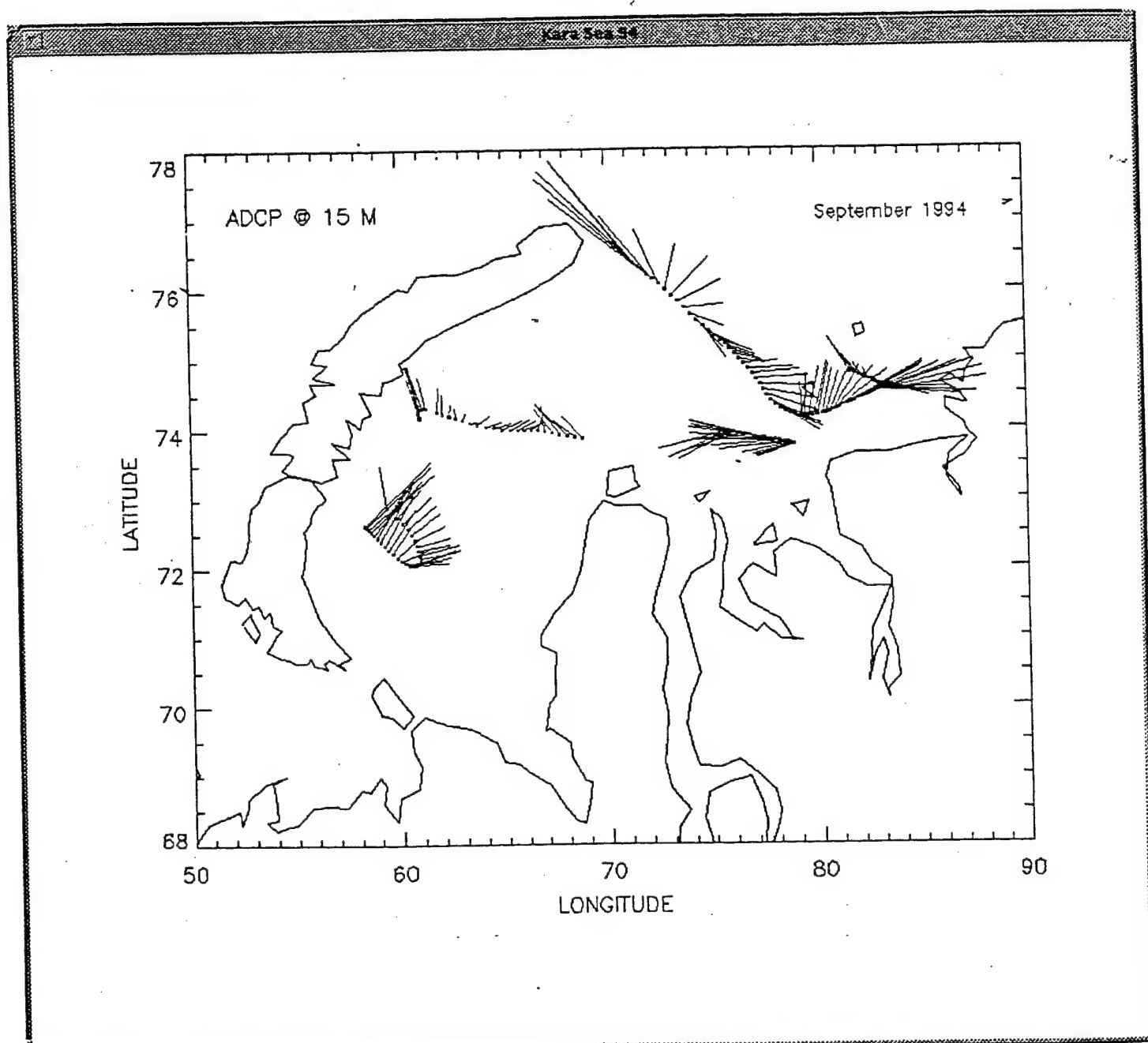


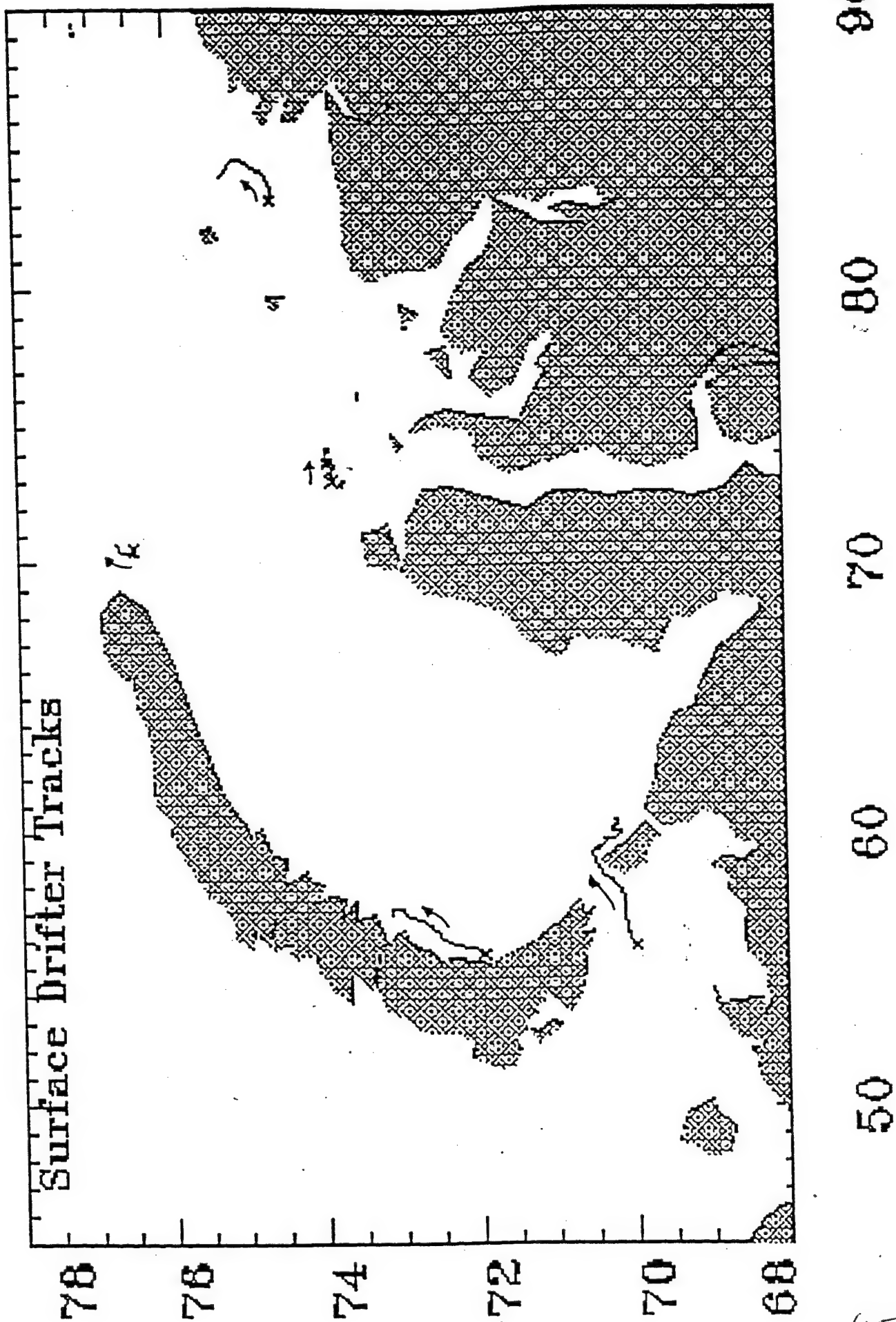


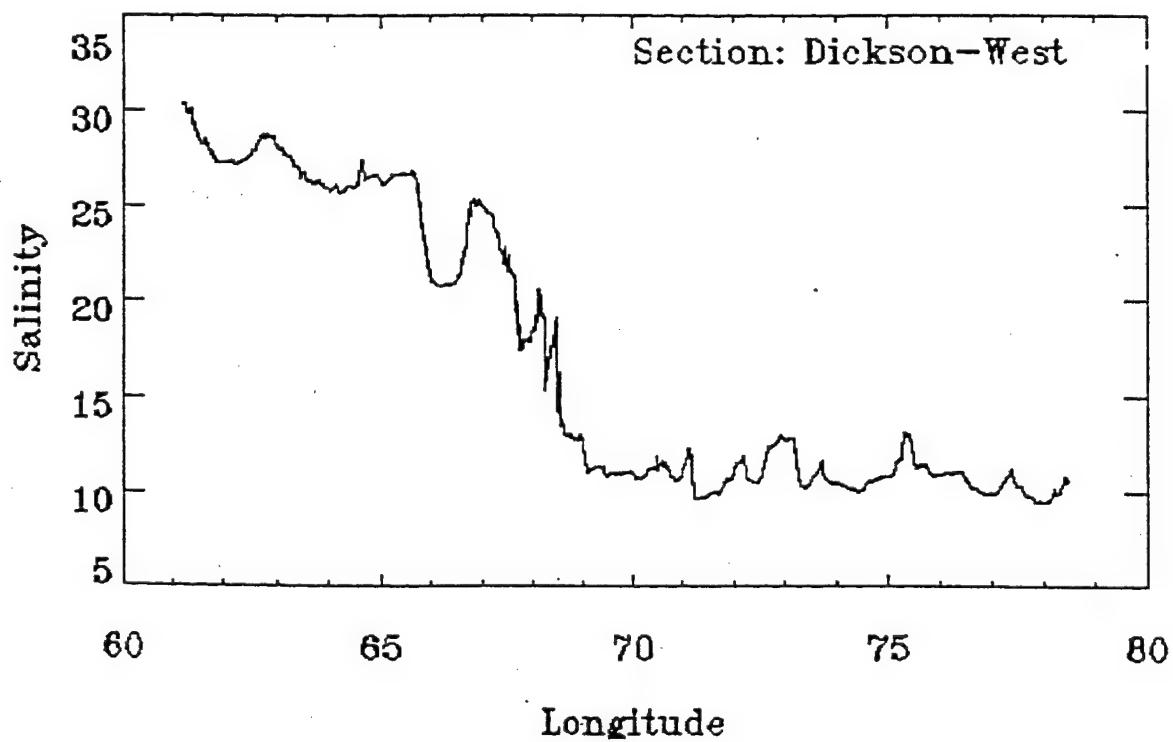
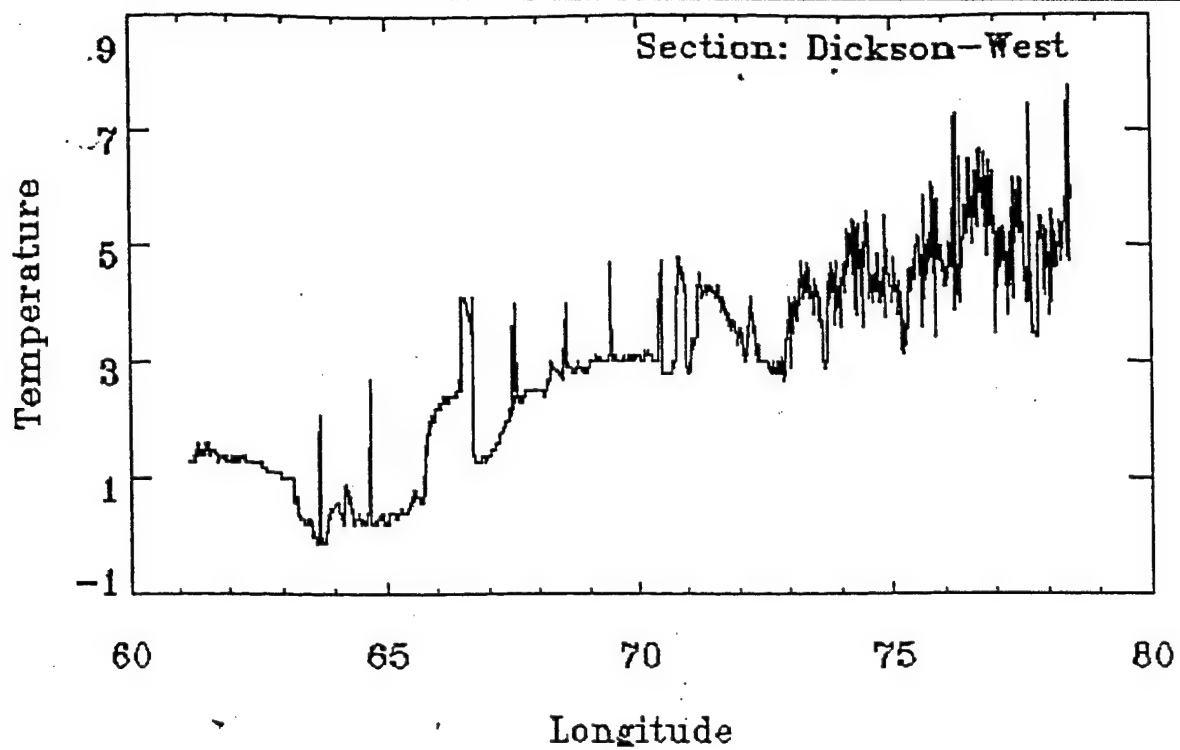
M2 Tide - 12.42 hr
Inertial - 12.5 hr
 \therefore Averaged over 12.5 hr

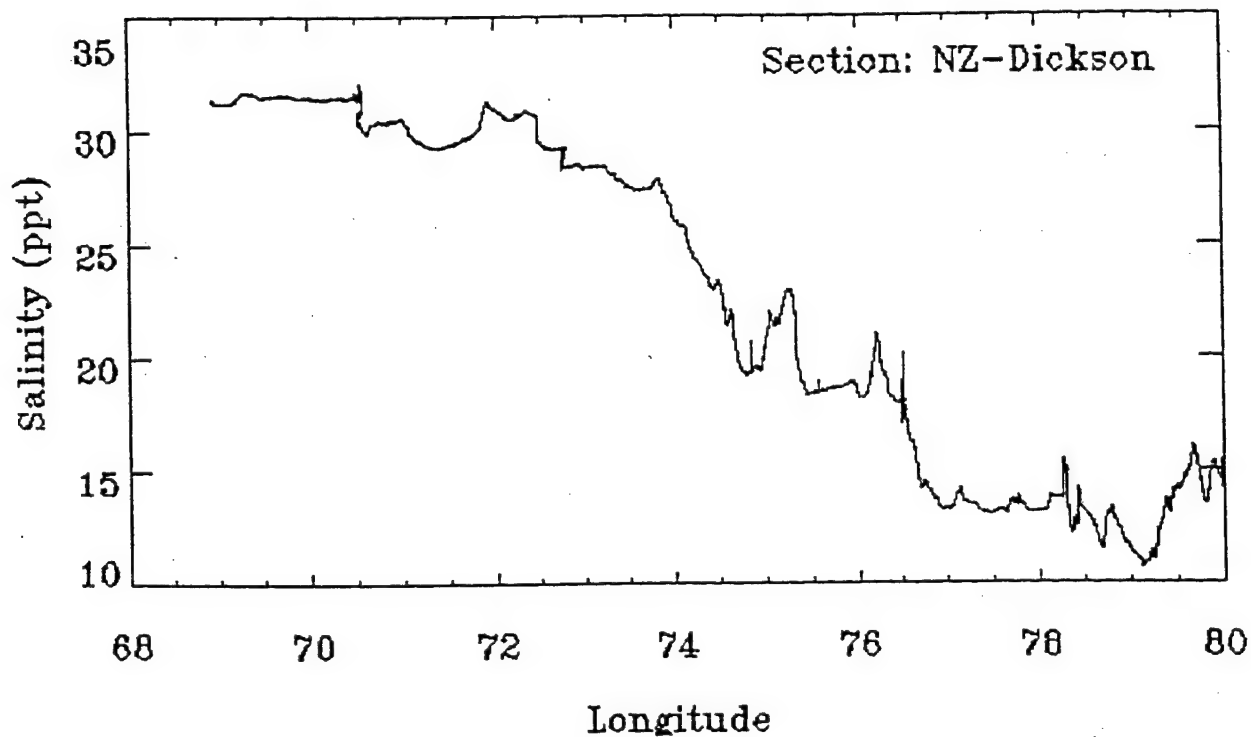
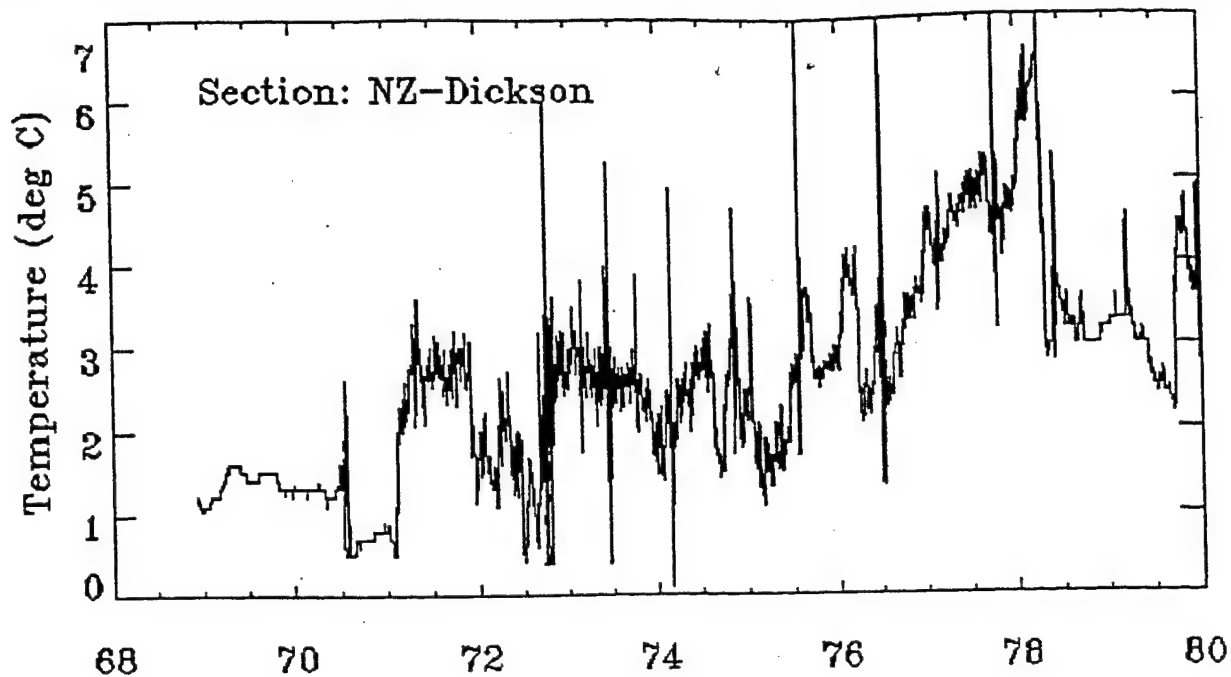


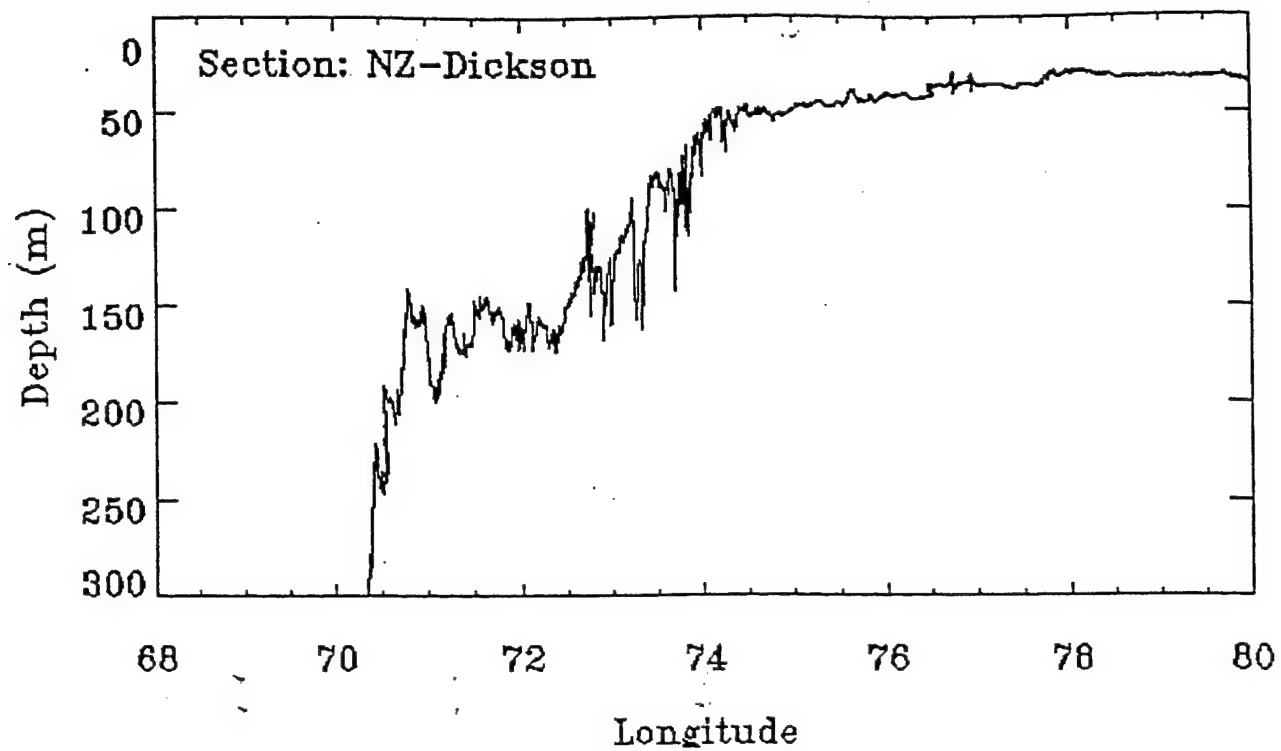
102'











scales

$$\text{Coriolis } f = 2.25 \text{ e}^{-05}$$

$$\delta\rho = 13.9 \text{ e}^{-03}$$

$$h = 20 \text{ m}$$

$$c_i = 83 \text{ cm/s}$$

$$\text{Radius of deformation: } \lambda_i = 37 \text{ km}$$

$$A_h = 1.0 \text{ e}^{+06 \text{ to } +08} \text{ cm}^2/\text{s}$$

$$L_{sb} = 170 \text{ km}$$

$$\text{Time to spread: } 300 \text{ to } 30 \text{ days}$$

Wind/current vector correlation data

$$w1xw2*=[re+i(im)]/[sqrt(s1)xsqrt(s2)]$$

$$\text{where } re = \text{sum}(u1xu2+v1xv2)$$

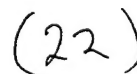
$$im = \text{sum}(v1xu2-v2xu1)$$

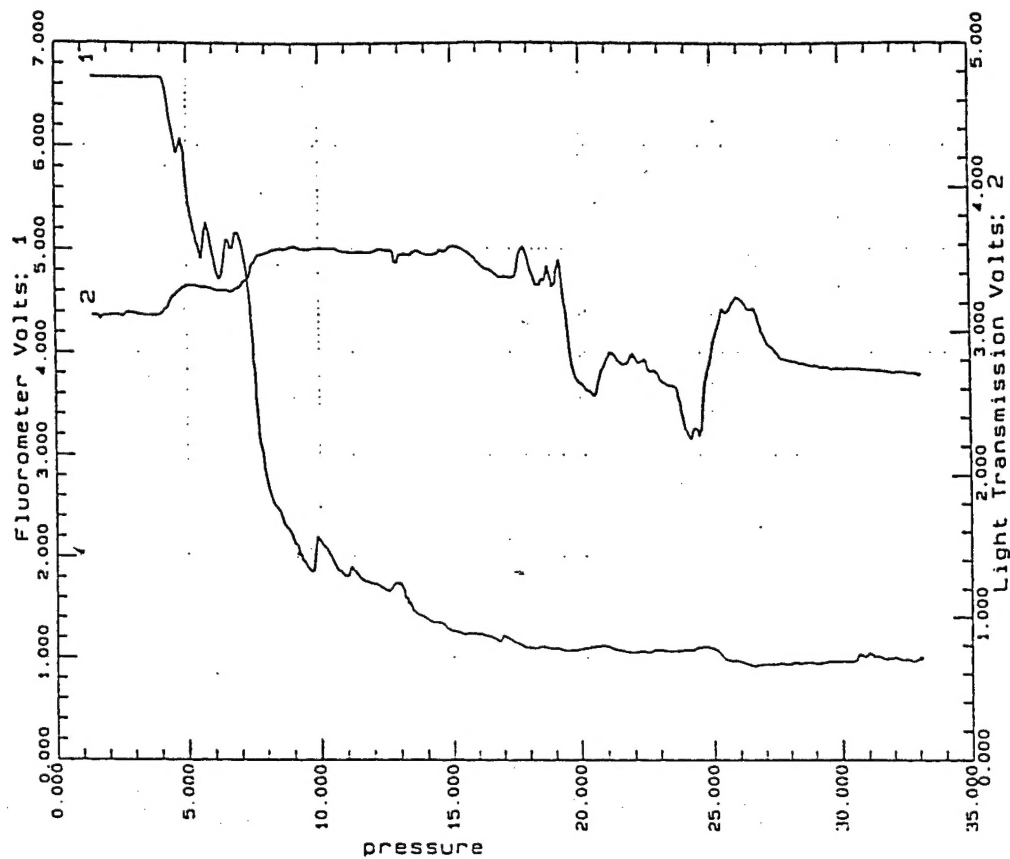
$$s1 = \text{sum}(u1xu1+v1xv1)$$

$$s2 = \text{sum}(u2xu2+v2xv2)$$

mooring	npts	r	phi(degrees)
404s	40	.63	91
406s	31	.14	59
409s	30	.40	70
421s	23	.27	64
422s	20	.58	48
429s	27	.62	86

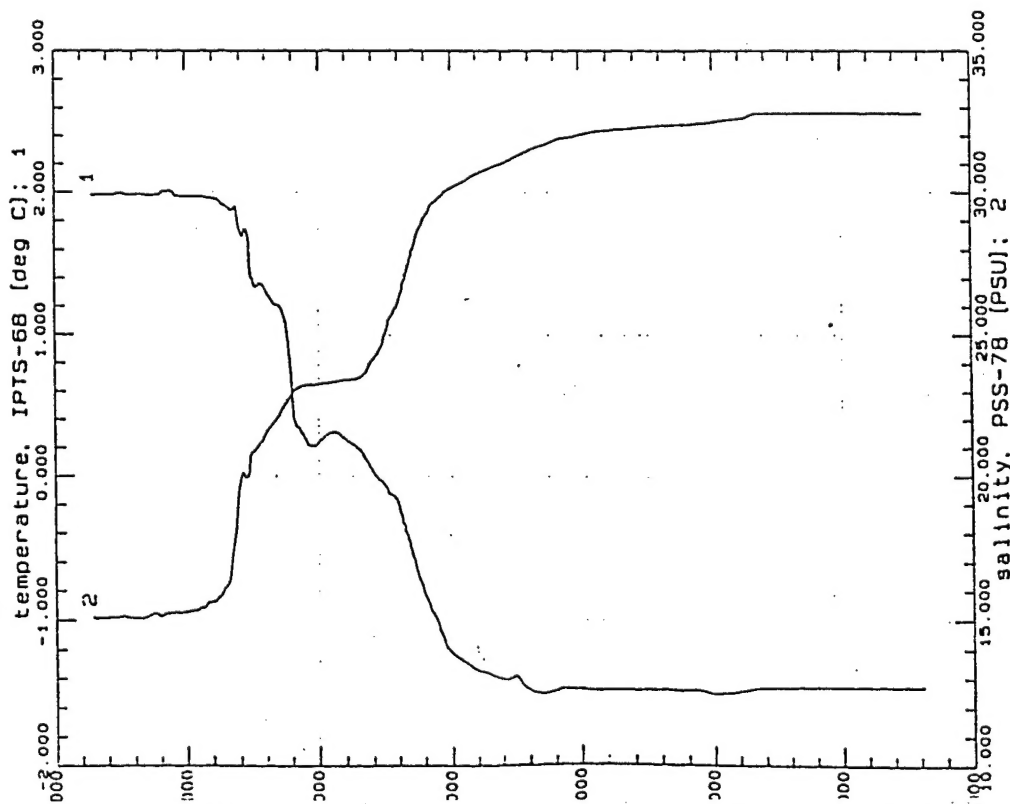
Note: correlation between 12.5 hour averages.
 Inertial Period (74 deg): 12.48 hr
 Semi-daily tides: 12.42 hr.





6.13b

09120750.CNV: 100 Km North of Ob/Yenisey



6.12a

09120750.CNV: 100 Km North of Ob/Yenisey

11/

CONCLUSIONS

1. The Kara Sea contributes about 1/2 the fresh water inflow to the Arctic. This makes it extremely important from physical dynamics as well as from Arctic pollution concerns, especially since the drainage basins of the contributing rivers are industrialized.
2. Vigorous mixing from tides, inertial currents and winds spread the river outflow toward the west as well as toward the east as expected from fluid dynamics on a rotational earth.
3. This westward spreading was confined in 1994 due to a relatively strong current along the slope of the Yamal Plateau.
4. Flow along the eastern side of Novaya Zemlya was northward, instead of southward as expected.
5. Flow around the northern tip of Novaya Zemlya appeared to be northwestward, instead of southeastward, into the Sea, as expected. However, without longer time series, this cannot be justified as characteristic, even over the short summer time.
6. We need to better understand the pathways for spreading of Kara Sea fresh water into the rest of the Arctic.